Pergamon

Building and Environment, Vol. 32, No. 5, pp. 447–4
© 1997 Elsevier Science Ltd. All rights
Printed in Grea
0360–1323/97 $17.(

AIVC 10779

PII: S0360–1323(97)00006–1

A Novel Thermal Simulation Model and its Application on Naturally Ventilated Desert Buildings

E. H. MATHEWS*
Y. ETZION†
E. VAN HEERDEN*
S. WEGGELAAR*
E. ERELL†
D. PEARLMUTTER†
I. A. MEIR†

(*Received* 28 *August* 1996; *revised* 2 *October* 1996; *accepted* 21 *January* 1997)

A new thermal simulation model, QUICK II, is presented and numerous verification case studies performed on naturally ventilated buildings are discussed. Four new case studies performed on two buildings located in the Negev desert in Israel are discussed in detail. All the measurements pertaining to these new case studies were taken independently by the Desert Architecture Unit of the Jacob Blaustein Institute for Desert Research. These measurements are provided, along with a description of the buildings. The verification results show a good correlation between the measured and simulated parameters. The simulated temperatures were found to be within 1°C of the measured temperatures for 73% of the time, and within 2°C for 95% of the time. © 1997 *Elsevier Science Ltd.*

NOMENCLATURE

A	area [m^2]
C	thermal capacitance [J/°C]
C_P	specific heat capacity at constant pressure [J/kg °C]
h	convective heat transfer coefficient [W/m^2 °C]
I	incident radiation [W/m^2]
Q_c	convective heat load [W]
Q_r	radiative heat load [W]
R	thermal resistance [°C/W]
T	temperature [°C]
Vol	volume [m^3]
α	absorbtivity
ϵ	emissivity
ρ	density [kg/m^3]

Subscripts

a	air
e	external
hm	high mass
i	internal
im	internal mass
lm	low mass
o	outside
s	surface
sa	solar air
ss	steady state
v	ventilation

INTRODUCTION

The thermal simulation method originally developed by Mathews [1] and implemented in QUICK was meant for completely passive buildings. The original model [2, 3] was a first-order model. The most important shortcomings of first-order models for building zones are that they do not adequately represent the thermal response of thermally thick elements or intermittent interior heat loads.

The original model obtains very good results for completely passive buildings where no heat sources are present in the building zone. Good results are also obtained for buildings with continuously applied internal loads. While passive buildings can be simulated very accurately, less accurate results have been obtained for buildings equipped with air-conditioning, or intermittent heat loads. For some verification calculations, the results obtained from the first-order model and numerically predicted values were found to differ.

Verification should be seen as an integral part of the model development process, and should command its fair share of resources and intellectual effort [4]. Verification

*Centre for Experimental and Numerical Thermoflow, Department of Mechanical Engineering, University of Pretoria, Pretoria, South Africa.

†Desert Architecture Unit, Jacob Blaustein Institute for Desert Research, Ben-Gurion University of the Negev, Sede-Boker Campus, Israel.

E. H. Mathews, E. van Heerden and S. Weggelaar are also consultants to Transfer of Energy, Momentum and Mass (TEMM) International (Pty) Ltd.

is often neglected, however, due to the lack of a well-defined methodology and the difficulties involved in obtaining good data sets. The amount of time spent on verifying analysis programs in the building industry is almost negligible in comparison with the time spent by program developers from other disciplines [5].

QUICK II has been extensively verified on South African buildings, but since independent verification provides unbiased evaluation it was decided to verify buildings in the northern hemisphere as well. TEMM International, the developers of QUICK II, and the Desert Architecture Unit, have previously worked together in validating the original model [6]. The ongoing research being conducted in the Negev desert provides valuable independent verification data.

THERMAL MODEL

The occurrence of discrepancies between the results obtained from the first-order model and numerical predictions prompted further investigation into an extension to a higher-order model. A theoretically rigorous procedure was followed to determine the heat flow in a building zone. Firstly, the heat flow through a single wall was considered. The heat flow through several walls was then added to obtain the total heat flow in the zone. At this stage of the procedure, the radiative and convective heat generated in the zone had not yet been included. The use of an electrical analogy for this purpose is introduced in this section (see Fig. 1).

It can rightfully be asked why an electrical analogy is required, if an analytical solution for the heat flow into a building zone already exists. The only reason for this is that in the analytical solution, it is assumed that the spectra of all the relevant parameters are known beforehand. This is not generally true for example when the calculation of the ventilation rate is dependent on the solution of the inside air temperature, or when the model is applied to the simulation of air conditioning plants.

It is therefore clear that another approach is required if the simulation model is to simulate the building zone with an air-conditioning plant and its controls. The recommended procedure is discussed in the following paragraphs. It must be noted that while the use of an electrical analogy in itself is not novel, the configuration of the electric circuit presented in this paper is.

The air node of the electric circuit is treated as a separate node, and its capacitance (C_i) is simply calculated by

$$C_i = Vol*\rho*C_p,$$

where Vol is the zone volume, ρ is the air density and C_p is the specific heat capacity of the air. The ventilation, infiltration and environmental control are all treated separately and the resistance is given as

$$R_v = 1/(Vol*\rho*C_p*acs),$$

where *acs* is the air changes per second. These *acs* values for natural ventilation are obtained by the calculation procedure suggested by Rousseau and Mathews [7].

Provision is made for two structural heat flow paths, namely: (1) a low mass path (single node-glass, fenestration and other low mass structures), and (2) a high mass path (triple node). The thermal resistances and capacitances for the high and low mass paths are determined by optimization. The analytical solution in the frequency domain is determined from the theory derived by Davies [8]. The response of the electrical analogy is then matched to the analytical solution by selecting values for R and C. The details of this procedure will form the basis of a separate article.

In other models the low mass structural heat flow path is often represented by a resistor only [9]. The procedure here is different, thus allowing thermally thicker elements to be included in the low mass path. A thermally thicker element is one for which a large product is obtained when the thermal resistance of the element is multiplied by the thermal capacity of the element. Surface convective resistances are calculated by

$$R_s = 1/(h_i A_s),$$

and the solar-air temperature is calculated by

$$T_{sa} = T_o + (\alpha I_s - \epsilon I_l)/h_o.$$

For the ground contact model, the calculation procedure suggested by Richards and Mathews [3] was used.

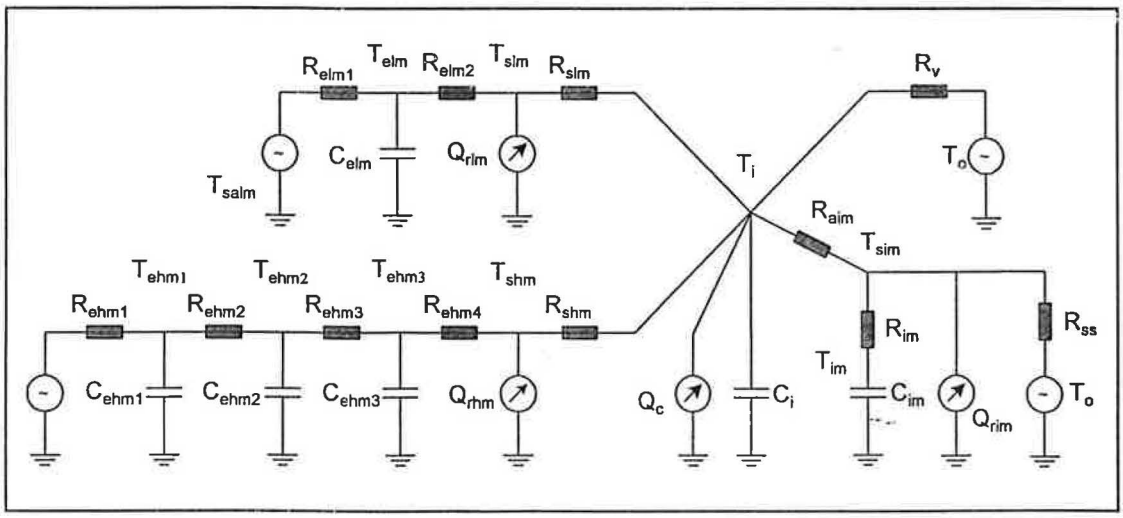

Fig. 1. Zone model electrical analogy.

All internal masses are combined and treated as a single capacitor. This internal mass capacitance, C_{im}, accounts for the heat storage effect of the floor and internal masses, and is simply calculated as the sum of all the capacitances. The thermal resistance, R_{im}, is calculated by determining firstly the time constants for each internal mass, and then the effective resistance. The steady state resistance, R_{ss}, accounts for the heat that is lost from the floor to the surrounding environment. A detailed discussion of this procedure can be found in [3].

Convective heat gains, Q_c, resulting from internal convective heat sources, act directly on the air node. Radiative heat gains, Q_r, resulting from solar penetration and internal radiative heat sources, are weighed according to surface area and act directly on the surface.

The governing equations for the complete circuit can be derived by adding the currents at each node. In total, the circuit contains nine nodes. Six of the nodes are associated with capacitors, and the other three with surfaces. The differential equations resulting at the nodes containing capacitors can be discretized using a forward differencing scheme. The use of heat balances at the surfaces contributes three algebraic equations containing the surface temperature terms.

The resulting nine equations must be solved simultaneously at each time step. Although this is a considerable complication (when considering the original [2, 3] or other low-order models such as that proposed by Tindale [9]), the increase in accuracy should justify the effort. While the task might seem formidable, the resulting matrix is sparse with an almost tri-diagonal structure. Most of the coefficients remain constant, allowing the matrix to be inverted only once. This data is then stored. As a result, only the backward substitution needs to be performed at each time step. This can be done very efficiently.

VERIFICATION

Background

The success of any building thermal model lies in its successful verification. Analytical and inter-model verification are both important when verifying a new model, but empirical validation is essential. Empirical validation is the most powerful of the validation tools, because it provides a direct measure of truth of the simulation model against reality [10].

Validation studies were originally performed in 32 building zones in various types of buildings. The 32 zones comprised four experimental huts, three residential bedrooms, a bathroom, a residential garage, two dormitories, a prefabricated unit, a shop, two school classrooms, two storerooms, a showroom, a church, a factory and 12 offices. A validation study conducted over such a wide range increases confidence in the model's applicability in practice.

To extend the study, a number of the original zones were modified by adding insulation, changing exterior colors, opening and closing windows, etc. The modification brought the total number of zones validated to 70. Although most of the zones formed part of multizone buildings, only 11 studies were simulated as multizone experiments.

Verification parameters

When validating the thermal model, it is impossible to consider each study individually. For this reason, criteria need to be established to facilitate the evaluation of the model. In this section, three global parameters which enable us to evaluate all the data are defined. The three global parameters are: (1) the mean indoor temperature, (2) the indoor temperature swing and (3) the phase shift between the measured and predicted indoor air temperatures.

Calculation of the three parameters is elementary. Firstly, the mean indoor air temperature is simply the mean of the hourly values for the 24 hour period. Secondly, the indoor temperature swing is calculated as the difference between the maximum and minimum indoor temperatures. Finally, to determine the phase shift, the time differences between the measured and predicted indoor maxima, and the measured and predicted indoor minima are calculated. The phase shift is then calculated as the mean of these two values.

The predicted and measured indoor temperature means obtained for the 70 case studies using the new third-order model are shown in Fig. 2. The correlation coefficient obtained was 0.993. The predicted and measured temperature swings for the 70 case studies using the new third-order model are shown in Fig. 3. The correlation coefficient obtained was 0.956.

It can be seen from the preceding figures that a good correlation was obtained in both cases. The correlation obtained for the measured and predicted temperature swings is lower than that obtained for the mean indoor temperatures, but is still acceptable for a design tool.

The cumulative error distribution obtained for the 1680 temperatures simulated during the 70 case studies is shown in Fig. 4.

It is clear from Fig. 4 that the cumulative error distribution obtained is very pleasing. The indoor temperatures were predicted within 1°C of the measured temperatures for 73% of the time, and within 2°C for 95% of the time.

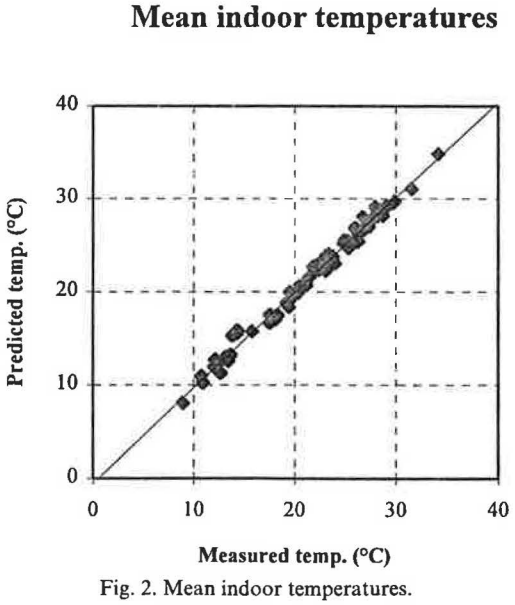

Fig. 2. Mean indoor temperatures.

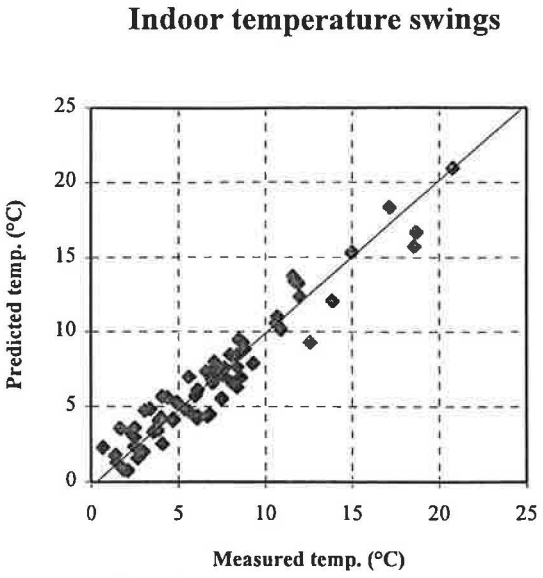

Fig. 3. Indoor temperature swings.

MEASUREMENTS

Introduction

In addition to the original verification studies, independent verification studies were also conducted by the Desert Architecture Unit of the Jacob Blaustein Institute for Desert Research. These studies will be discussed in this section.

Four verification studies were performed in total, two on a lightweight building and two on a conventional heavy building. For the lightweight building, only one scenario—windows open and unshaded throughout the day—was investigated for two separate measurement periods. For the heavy building, two scenarios were investigated for separate measurement periods, namely windows open and unshaded throughout the day and windows open and unshaded from 1700h to 0800h.

Detailed measurements were taken for each of the verification studies, including: (1) hourly outdoor temperature, humidity and global and diffuse radiation data, (2) hourly wind direction and wind velocity data, and (3) hourly indoor temperature data. Measurements for all the case studies were taken over a period of a week. The measured data in each set was then used to obtain an average day for each set. This average day can be seen as a design day representation of the actual measurements. See Tables 1 and 2.

While the majority of the required input parameters were measured, no infiltration or ventilation rates were measured. This deficiency in the measured data set will obviously have an effect on the results obtained. In a case such as this, however, where the analysis program is intended as a design tool, it must be remembered that accurate ventilation rates would not be available. These rates would thus have to be predicted, as is the case here.

Building description

Lightweight building The lightweight building used for verification purposes was a factory-built low mass, transportable residential building. The large number of immigrants entering Israel from the early 1990s created a massive demand for housing. This increased demand was not accompanied by an increase in capital investment and this placed great pressure on the building industry. As a result, the cost of housing increased and the government Ministry of Construction and Housing became directly involved in the planning and provision of housing [11].

The use of prefabrication became a major part of the housing provision strategy in order to control the costs and regulate production. The use of this technology was further prompted by government incentives for rapid completion of the housing units. The lightweight building illustrated in Fig. 5 is an example of the units which were ordered to provide temporary housing. The building measures 12.4 m by 3.7 m and the height (inside) varies from 2.25 to 2.45 m. The building is split into two independent units of equal size and is placed on short legs at a height of approximately 0.5 m above the ground.

The building's walls are made of steel structural elements with sandwich panels between them. The sandwich panels consist of, from outside in, a fiber board with a water repelling facing, 60 mm fiberglass insulation and gypsum board. The roof consists of white painted sheet metal, an air space, 100 mm of mineral wool insulation and a gypsum board ceiling. Furthermore, the roof is

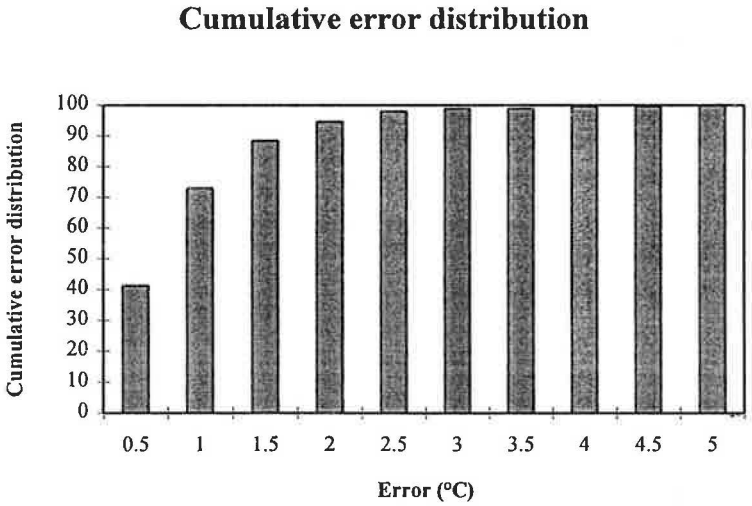

Fig. 4. Cumulative error distribution.

Table 1. Measured data for the period 18/8/92–25/8/92. Windows open and unshaded for both structures

Hour	Environmental conditions						Indoor conditions	
	$T_{OUTDOOR}$ (°C)	$RH_{OUTDOOR}$ (%)	RAD_{GLOB} (W/m²)	RAD_{DIFF} (W/m²)	v_{WIND} (m/s)	Wind direction (°)	T_{LIGHT} (°C)	T_{HEAVY} (°C)
1	20.0	74	0.00	0.00	1.9	289	21.9	25.6
2	19.7	74	0.00	0.00	1.4	264	21.7	25.4
3	19.3	75	0.00	0.00	1.2	261	21.4	25.2
4	18.9	75	0.00	0.00	1.3	265	21.0	25.0
5	18.5	76	0.84	0.59	1.1	237	20.7	24.9
6	18.8	75	67.90	45.57	1.3	255	20.4	25.1
7	20.8	65	249.01	160.08	1.7	234	20.8	25.4
8	23.0	59	453.38	283.88	2.0	268	22.2	25.9
9	24.3	55	677.79	409.97	2.2	284	24.1	26.5
10	26.0	52	791.27	445.76	2.3	260	25.9	27.1
11	27.7	48	901.43	463.11	2.6	269	27.7	27.5
12	29.1	46	928.00	432.59	2.9	277	29.1	28.1
13	30.2	44	879.00	357.80	3.3	294	30.2	28.6
14	30.8	43	758.04	257.36	3.7	301	31.0	28.8
15	31.0	42	597.50	181.80	4.1	309	31.1	28.9
16	30.0	45	400.57	115.34	4.8	320	30.5	28.7
17	28.0	51	207.14	72.50	5.5	327	28.9	28.5
18	25.9	54	39.93	18.24	5.1	330	27.2	27.8
19	24.0	60	0.27	0.06	4.3	333	25.5	27.2
20	23.0	65	0.02	0.00	3.5	330	24.4	26.7
21	22.1	69	0.00	0.00	3.0	334	23.6	26.3
22	21.6	71	0.00	0.00	2.6	325	23.0	26.1
23	21.1	72	0.00	0.00	2.6	304	22.5	25.9
24	20.6	73	0.00	0.00	2.0	312	22.2	25.8

sloped at an angle of 15°. The insulating fiberglass mat floor is supported by XPM wire mesh and covered with PVC. All windows in the building are single glazed with aluminum frames and are positioned in long facades.

Heavy building The heavy structure used for verification purposes is a full-scale demonstration building of approximately 75 m² which was constructed as the final stage of a four-year research program on the use of

Table 2. Measured data for the period 24/8/92–30/8/92. Windows open and unshaded for both structures, but only between 1700 and 0800h for the heavy structure

Hour	Environmental conditions						Indoor conditions	
	$T_{OUTDOOR}$ (°C)	$RH_{OUTDOOR}$ (%)	RAD_{GLOB} (W/m²)	RAD_{DIFF} (W/m²)	v_{WIND} (m/s)	Wind direction (°)	T_{LIGHT} (°C)	T_{HEAVY} (°C)
1	20.0	76	0.00	0.00	1.5	268	22.2	25.0
2	19.6	76	0.00	0.00	1.2	279	22.0	24.9
3	192	77	0.00	0.00	1.0	270	21.4	24.7
4	18.8	77	0.00	0.00	1.0	273	21.1	24.5
5	18.5	77	0.00	0.00	0.8	241	20.8	24.3
6	18.4	77	51.33	34.10	0.7	272	20.4	24.4
7	20.1	70	227.77	158.76	1.1	261	20.6	24.8
8	22.7	61	494.76	332.91	1.5	249	22.0	25.2
9	24.9	54	677.39	433.53	1.9	236	24.1	25.4
10	26.7	50	797.13	466.56	2.1	271	26.1	25.5
11	28.7	46	901.14	478.20	2.3	261	28.1	25.7
12	30.1	43	927.14	448.20	2.6	269	29.7	25.8
13	31.4	41	874.14	374.97	2.9	287	31.0	26.0
14	31.8	41	749.76	272.57	3.2	291	31.5	26.1
15	32.2	40	581.26	187.41	3.9	306	31.9	26.2
16	30.5	45	371.22	112.80	4.8	318	30.9	26.2
17	28.8	49	190.45	67.66	5.1	322	29.6	26.7
18	26.6	53	29.72	14.29	5.2	325	27.9	26.7
19	24.6	59	0.00	0.00	4.8	327	26.1	26.2
20	23.2	66	0.00	0.00	4.1	331	24.9	25.8
21	22.3	70	0.00	0.00	3.3	334	23.8	25.6
22	21.6	72	0.00	0.00	2.7	324	23.3	25.4
23	20.9	74	0.00	0.00	2.1	303	23.0	25.3
24	20.4	75	0.00	0.00	1.6	297	22.7	25.2

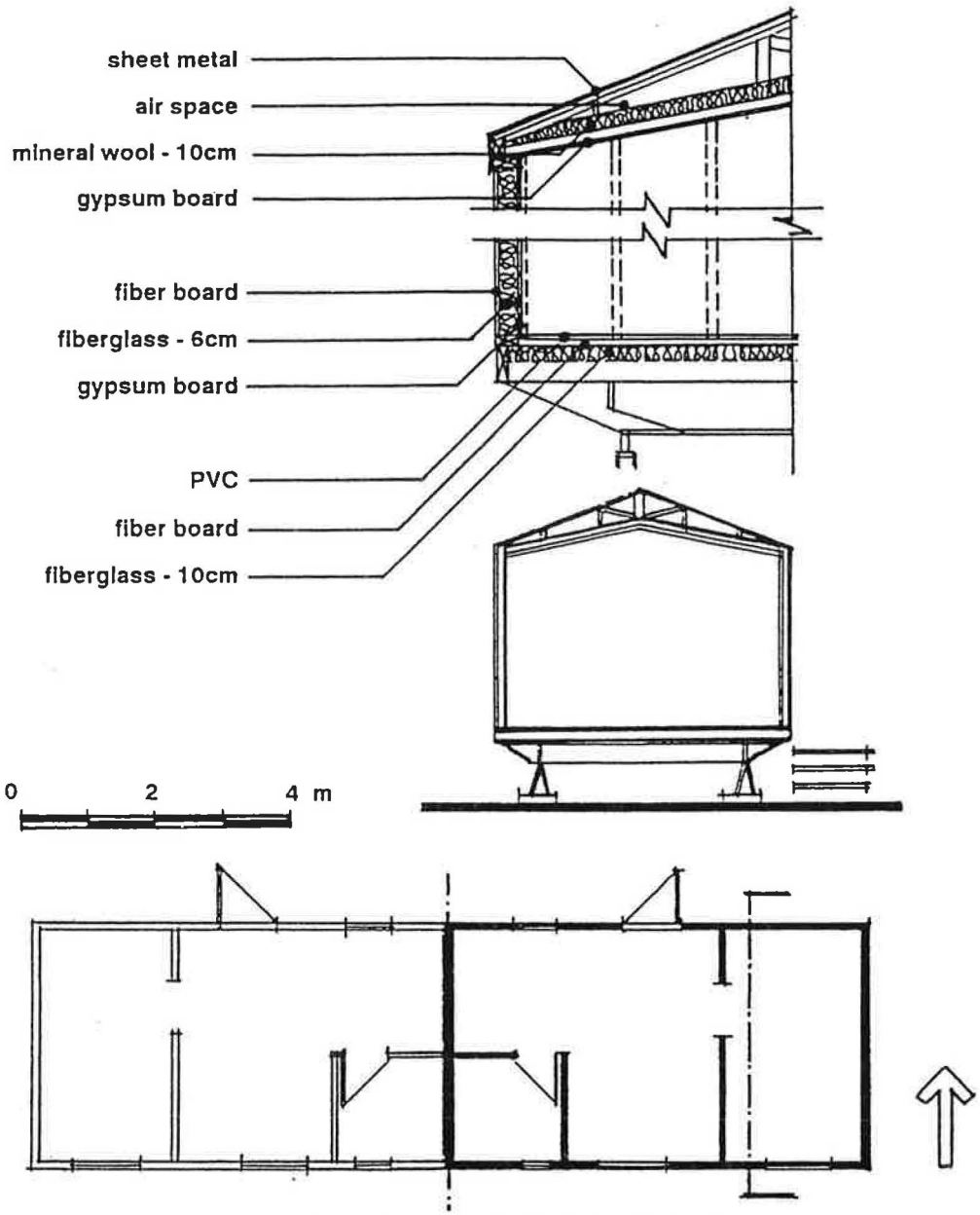

Fig. 5. Plan, section and detail of the lightweight building.

radiative cooling systems in desert regions. As can be seen from the building layout in Fig. 6, the building consists of a number of rooms.

Two of the larger rooms (east and west) were used to test the two systems which had been designed previously, while the third larger room (south) was used as a reference room. Only this reference room was used for verification purposes, and the room is highlighted on the building layout.

The building walls consist of a 200 mm silica block, insulated externally with 50 mm expanded polystyrene faced with acrylic plaster. The roof consists of a 150 mm reinforced concrete slab topped with a layer of foamed concrete and insulated with 100 mm expanded polystyrene. The floor comprises only a 150 mm reinforced concrete slab. All windows of importance are single glazed and are equipped with an external roller shutter.

VERIFICATION SIMULATION RESULTS

Once all the required data was fed into the simulation program, the indoor temperature profiles of two structures were simulated. The agreement between the model predictions and the actual measurements is affected by the quality of the data available on building characteristics and the weather, the absence of errors in inputting the above data, and the ability of model algorithms to correctly model physical processes.

The results obtained for the lightweight building are shown in Figs 7 and 8. The scenario for both verification studies was the same and this can be seen from the measured profiles. The results obtained for the conventional heavy building are shown in Figs 9 and 10. In this case, the scenario differed for the two verification studies. For the first case study, all windows in the zone were open

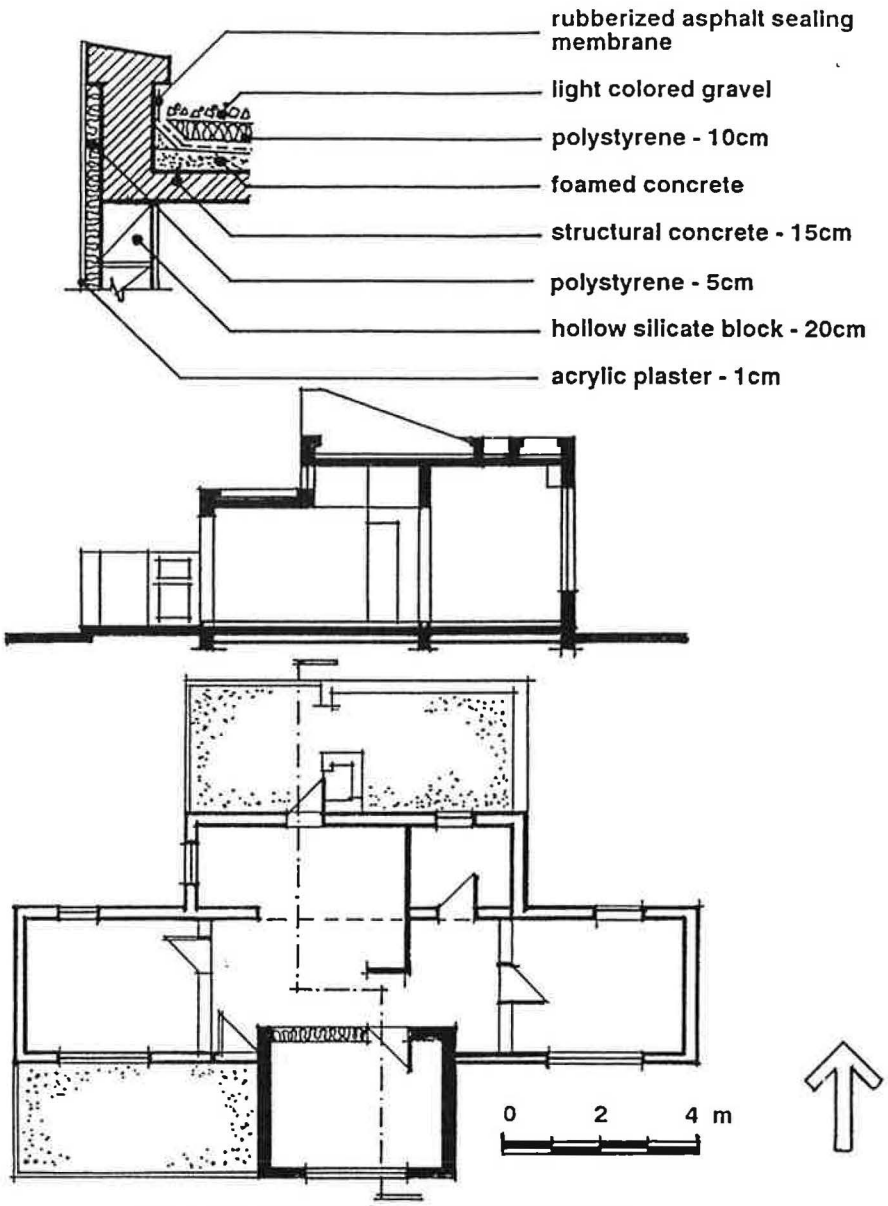

Fig. 6. Plan, section and detail of the conventional heavy building.

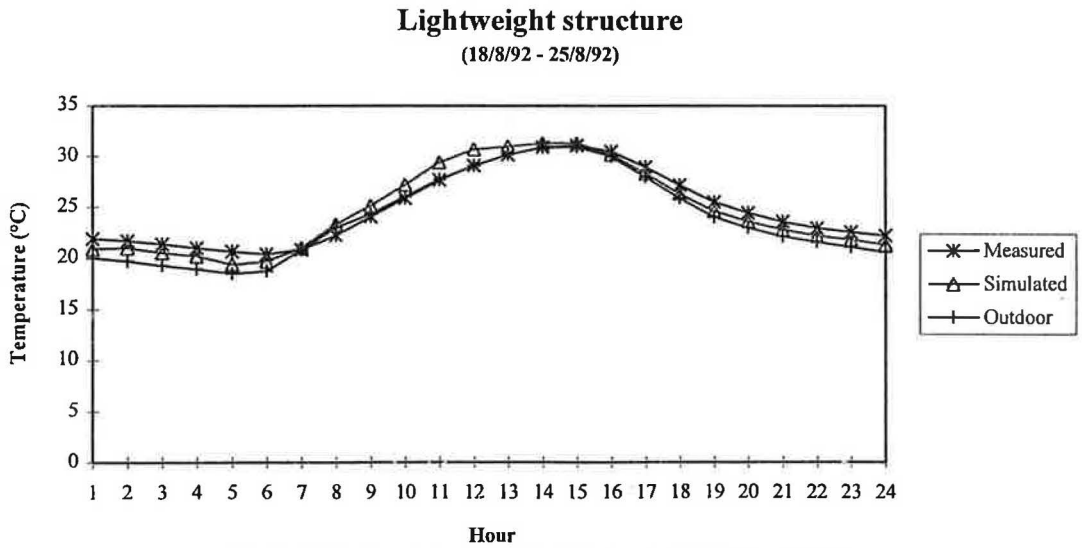

Fig. 7. Verification study for lightweight structure (18/8/92–25/8/92).

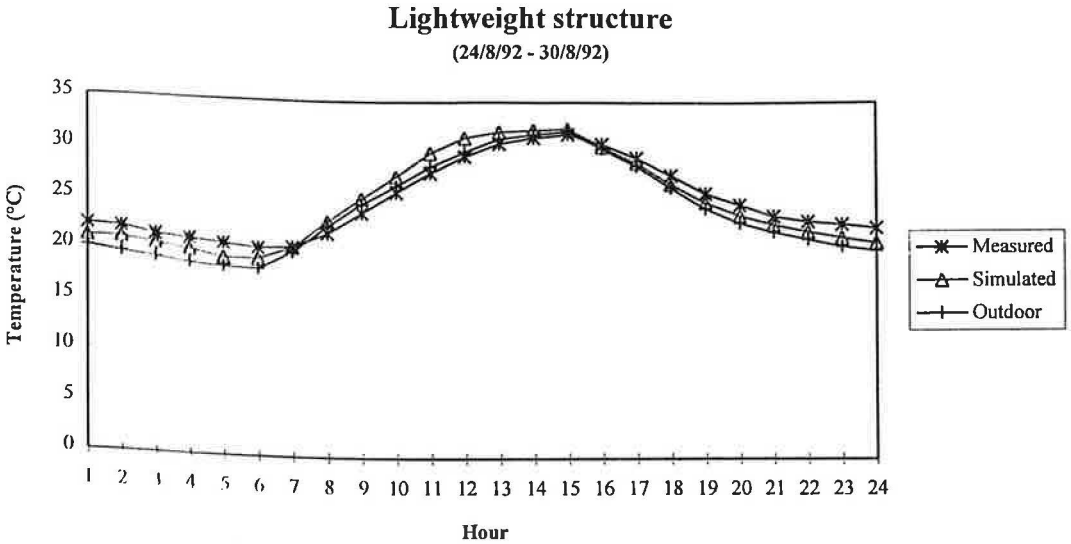

Fig. 8. Verification study for lightweight structure (24/8/92–30/8/92).

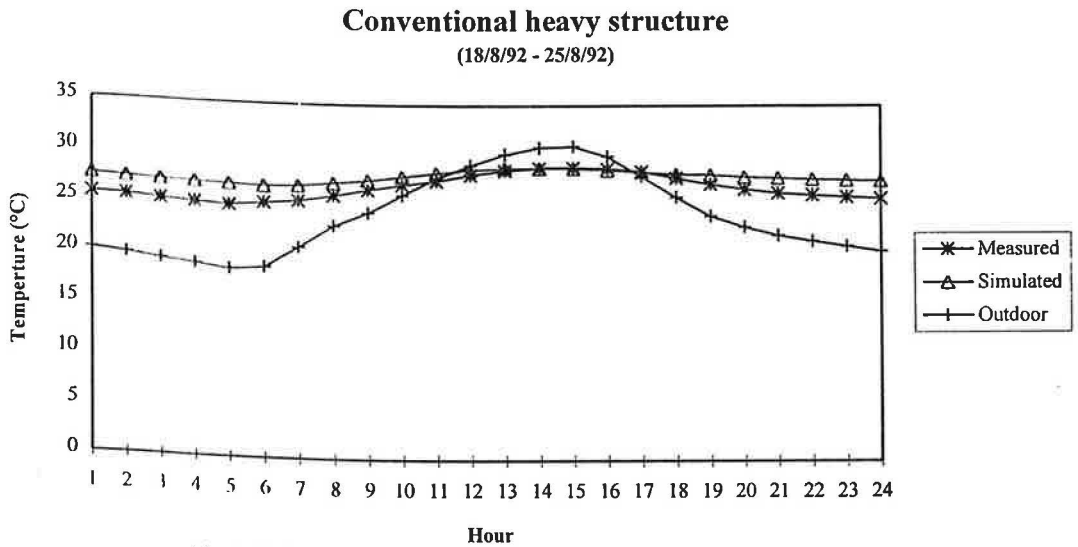

Fig. 9. Verification study for conventional heavy structure (18/8/92–25/8/92).

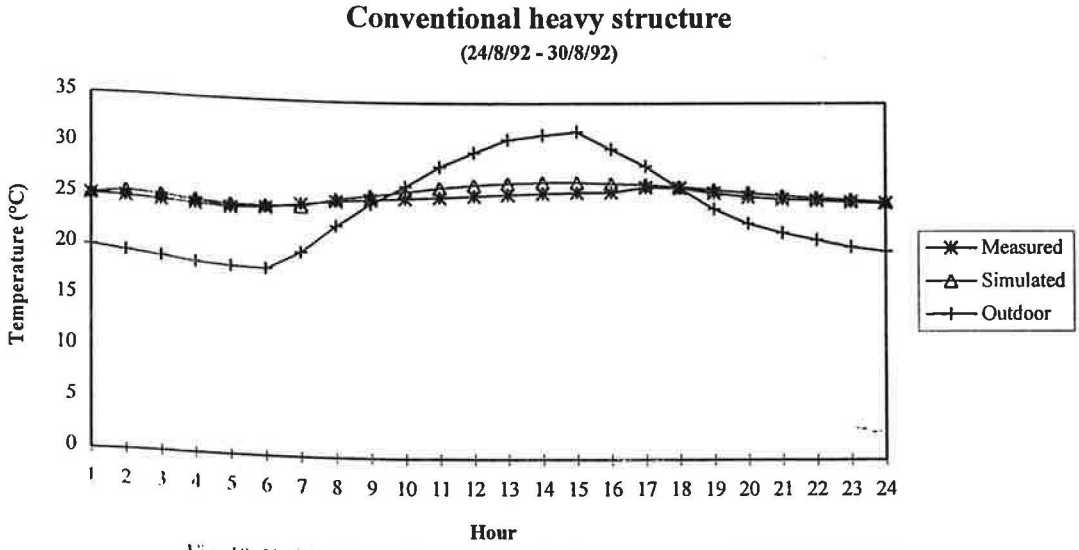

Fig. 10. Verification study for conventional heavy structure (24/8/92–30/8/92).

Table 3. Summary of simulation results

Scenario	Lightweight building				Conventional heavy building			
	1		2		1		2	
	Measured	Predicted	Measured	Predicted	Measured	Predicted	Measured	Predicted
Swing (°C)	10.7	11.9	11.5	13.0	4	2.0	2.5	2.6
$T_{AVERAGE}$ (°C)	24.9	24.7	25.2	25.0	26.7	27.8	25.5	26.0
Max. error (°C)	1.7		1.9		2.1		1.1	

and unshaded throughout the day, while for the second case study, the windows were open and unshaded only between 1700 and 0800h.

The simulated profiles for the lightweight building compare well to the measured profiles. In both verification studies performed on the lightweight building, the predicted temperature swing was slightly larger than the measured swing. This could be as a result of the sensitivity of the model to ventilation rates. It is important to remember that the ventilation rates used here are calculated by the program's ventilation model. Ideally these ventilation rates should be accurately measured.

Accurate calculation of the ventilation rates relies heavily on the use of the correct discharge coefficient for the windows of the building. Since the exact value of the discharge coefficient was not known, a typical value for this type of application was used, namely 0.6. Typical values of discharge coefficients for inlet openings vary between 0.5 and 0.9 [12] depending on the application. Values for outlet openings can be calculated [13]. High discharge coefficients will result in higher ventilation rates and vice versa.

To illustrate this, additional simulations were performed for the second lightweight scenario using discharge coefficients of 0.5 and 0.9. For the original simulation, the simulated air change rates varied between 4.2 and 56.3 air changes per hour (ach). By contrast, air change rates of between 3.6 and 46.9 ach were obtained for a discharge coefficient of 0.5. Similarly, air change rates of between 6.2 and 84.3 ach were obtained for a discharge coefficient of 0.9. This clearly illustrates the effect of varying discharge coefficients on the simulated air change rates.

Air change rates as high as those obtained for the lightweight scenarios will cause the indoor temperatures to be very close to the outdoor temperatures. This is reflected in the fact that the indoor temperatures are within 0.3°C of the outdoor temperatures at the time of maximum air change rates. Since these temperatures are already so close to each other, one would expect that the greatest effect of changing the discharge coefficients would be seen at the lower air change rates. By increasing the discharge coefficient to 0.9, a temperature difference of 0.4°C was obtained at these lower air change rates.

To a lesser degree, the ventilation rates are also affected by the building density in the surrounding area, and the specific location of the surrounding buildings. While the simplified ventilation model used here can account for the building density in the surrounding area, no provision is made for the specific location of the surrounding buildings.

High ventilation rates would cause the indoor temperature to tend towards the outdoor temperature. If the ventilation rates were calculated too high, it would account for the predicted temperatures being lower during the night. This could thus partly account for the discrepancies encountered between the measured and predicted minima.

The simulated profiles for the conventional heavy building compare well to the measured profiles. When the uncertainties in the underlying assumptions are considered, the results are seen to be satisfactory for a design tool. The simulation results are summarized in Table 3.

CONCLUSION

In this article, a novel thermal simulation model was introduced. The new model makes provision for all the major heat flow paths. Indoor temperatures for numerous verification studies have been accurately simulated. The temperatures simulated during the 70 case studies were found to be within 1°C of the measured temperatures for 73% of the time, and within 2°C for 95% of the time.

Measurements taken independently by the Desert Architecture Unit of the Jacob Blaustein Institute for Desert Research were used to further verify the simulation model developed by TEMM International. The simulated temperature profiles obtained compare well to the actual measured profiles. These results provide TEMMI with increased confidence in the model, and the fact that it can be used as a thermal design tool.

REFERENCES

1. Mathews, E. H., Thermal analysis of naturally ventilated buildings. *Building and Environment*, 1986, **21**, 35–39.
2. Mathews, E. H. and Richards, P. G., An efficient design tool for future building design. *Building and Environment*, 1993, **28**, 409–417.
3. Richards, P. G. and Mathews, E. H., A thermal design tool for buildings in ground contact. *Building and Environment*, 1994, **29**, 73–82.
4. Wiltshire, T. J. and Wright, A. J., Advances in building energy simulation in the UK—the Science and Engineering Research Council's programme. *Energy and Buildings*, 1988, **10**, 175–183.

5. Mathews, E. H., Shuttleworth, A. G. and Rousseau, P. G., Validation and further development of a novel thermal analysis method. *Building and Environment*, 1994, **29,** 207–215.
6. Mathews, E. H., Etzion, Y., Erell, E., Richards, P. G. and Rousseau, P. G., Simplified analysis of naturally ventilated desert buildings. *Building and Environment*, 1992, **27,** 423–432.
7. Rousseau, P. G. and Mathews, E. H., A new integrated design tool for naturally ventilated buildings. *Energy and Buildings*, 1996, **23,** 231–236.
8. Davies, M. G., Transmission and storage characteristics of walls experiencing sinusoidal excitation. *Applied Energy*, 1982, **12,** 269–312.
9. Tindale, A., Third-order lumped-parameter simulation method. *Building Services Engineers Research and Technology*, 1993, **14,** 87–97.
10. Irving, A. D., Validation of dynamic thermal models. *Energy and Buildings*, 1988, **10,** 213–220.
11. Pearlmutter, D. and Meir, I. A., Assessing the climatic implications of lightweight housing in a peripheral arid region. *Building and Environment*, 1995, **30,** 441–451.
12. Mathews, E. H., The prediction of natural ventilation in buildings. Dissertation presented for the degree of Doctor of Engineering, Potchefstroom University for Christian Higher Education, Potchefstroom, 1985.
13. Aynsley, R. M., *et al.*, *Architectural Aerodynamics*. Applied Science, London, 1977, p. 203.